BB

ISSN 1344-3879
RIKEN-AF-NP-364

Low Energy Dipole Strength in Light Drip Line Nuclei

H. Sagawa, T. Suzuki, H. Iwasaki, and M. Ishihara

RIKEN
ACCELERATOR
RESEARCH
FACILITY

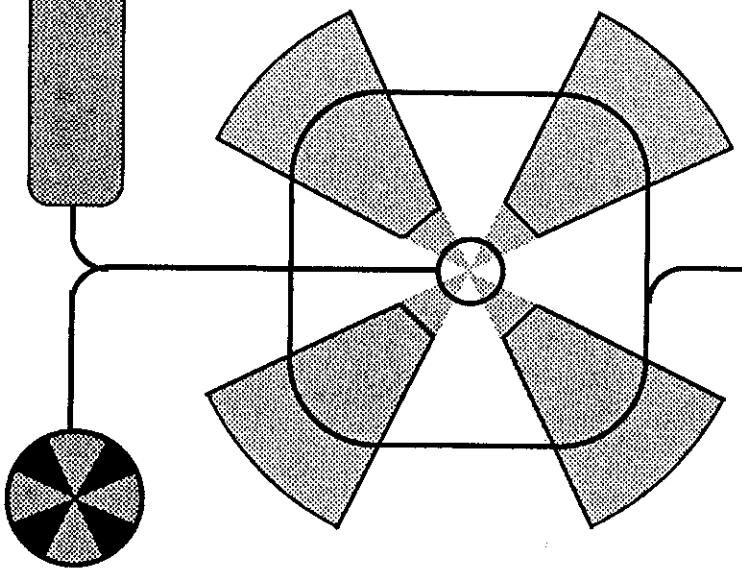

August 2000

The Institute of Physical and Chemical Research (RIKEN)
2-1 Hirosawa, Wako, Saitama 351-0198, Japan
TEL: (048)462-1111 FAX: (048)462-4642
e-mail: *username*@rikvax.riken.go.jp

Low Energy Dipole Strength in Light Drip Line Nuclei

H. Sagawa[1], Toshio Suzuki [2], H. Iwasaki[3] and M. Ishihara[4]

[1] *Center for Mathematical Sciences, the University of Aizu,*

Aizu-Wakamatsu, Fukushima 965-8580, Japan

[2] *Department of Physics, College of Humanities and Sciences, Nihon University,*

Sakurajosui 3-25-40, Setagaya-ku, Tokyo 156-8550, Japan

[3] *Department of Physics, University of Tokyo,*

7-3-1 Hongo, Bunkyo, Tokyo 113-0033, Japan

[4] *The Institute of Physical and Chemical Research (RIKEN), 2-1 Hirosawa, Wako,*

Saitama 351-0198, Japan

Abstract

We have studied electric dipole (E1) strength distribution in neutron and proton drip line nuclei ${}^{12}_{4}\mathrm{Be}_8$, ${}^{14}_{4}\mathrm{Be}_{10}$ and ${}^{13}_{8}\mathrm{O}_5$ by large scale shell model calculations with the effect of loosely-bound single particle wave functions. Large E1 strength are found in the low excitation energy region below E_x=3MeV in both ${}^{12}_{4}\mathrm{Be}_8$ and ${}^{13}_{8}\mathrm{O}_5$, while strong E1 strength are found only in high excitation energy region above E_x=7MeV in ${}^{14}_{4}\mathrm{Be}_{10}$. The effect of extended wave functions and the coherence in the transition amplitudes enhance significantly the E1 strength in the low energy region. A manifestation of melting of the shell magicity at N=8 and Z=8 is pointed out in the systematics of E1 transitions in Be- and O-isotopes.

21.60.Cs, 24.30.Cz, 25.20.-x

I. INTRODUCTION

Neutron and proton drip-line nuclei have been studied intensively because of its interesting exotic structure due to the loose binding of valence neutrons and protons [1–3]. In $^{11}_{3}Li_8$ and $^{11}_{4}Be_7$, these loosely-bound neutrons are called "halo" neutrons because of largely extended wave functions outside of the nuclear core. Much attention is paid now on electric dipole (E1) excitations in very low energy region of the nucleus with loosely-bound nucleons [4–10]. The E1 strength in stable nuclei is largely exhausted by giant dipole resonance (GDR), which is considered as a collective vibration mode constructed from a coherent superposition of particle-hole excitations crossing one major shell. The experimental excitation energy of GDR is found at E_x=$80/A^{1/3}$MeV, exhausting most of the sum rule strength, while the E1 strength in low energy region below 5 MeV is observed to be negligibly small in stable nuclei. It should be noticed that abnormally large E1 strength are confirmed experimentally in some light unstable nuclei in the low energy region below 5 MeV. The transition between the ground state with $J^{\pi}= \frac{1}{2}^{+}$ and the first excited $\frac{1}{2}^{-}$ state at E_x = 0.32 MeV in $^{11}_{4}Be_7$ is a well-known example of this anomaly, representing the strongest E1 transition ever observed between bound states [4]. A strong E1 transition to the bound 1^{-} state at E_x =2.68MeV is also found in $^{12}_{4}Be_8$ very recently [5]. Such strong E1 transitions may indicate a decoupled feature between the excitations of extended loosely-bound states and those of the core configurations [6]. The measurements of the low-lying E1 strength have been extended to the continuum excitations of neutron-rich nuclei $^{11}_{3}Li_8$ [7–9] and $^{11}_{4}Be_7$ [10], where the loosely-bound "halo" neutrons play an essential role to increase the strength.

Recently, the possible shell melting is often discussed in nuclei near drip lines, especially in relation with the magic numbers 8 and 20 [5,11–13]. Evidence of disappearance of magicity N=8 in $^{12}_{4}Be_8$ has been claimed recently from the study of proton inelastic scatterings [13] and Coulomb excitations on $^{12}_{4}Be_8$ [5]. The melting of the magic number N=20 was also pointed out experimentally in $^{32}_{12}Mg_{20}$ by the Coulomb excitations [14] as well as the early work on the excitation energy measurements of the first 2^{+} state [15].

The melting shell structure at the magic number 8 may be caused by much smaller energy gap between the p– and sd–shells than expected for the standard shell gap, i.e., $\hbar\omega = 41/A^{1/3}$MeV. The near degeneracy of $2s_{1/2}$ and $1p_{1/2}$ orbits relevant to the smaller energy gap may bring down a decoupled 1^- state at much lower energy than GDR energy region. Another possible effect of the shell melting is strong correlations among the valence nucleons outside of the core, which may cause a coherent effect in the transition amplitudes and enhance the low energy E1 strength largely. A shell model calculation of E1 strength in ${}^{11}_{3}Li_8$ at low excitation energy has been made in ref. [16], taking into account a large mixing of the two loosely-bound $(1p_{1/2})^2$ and $(2s_{1/2})^2$ configurations as well as the feature of extended wave functions. Indeed, the theory well explained the newly observed two peak structure in the E1 data of GSI [9]. The mixing of $(2s_{1/2})^2$ and $(1p_{1/2})^2$ configurations in the two loosely-bound neutrons has been found also important to explain the retardation effects of the Gamow-Teller (GT) transitions from ${}^{11}_{3}Li_8$ to ${}^{11}_{4}Be_7$ [17–19].

In this paper we will study the E1 strength distribution of two Be-isotopes ${}^{12}_{4}Be_8$ and ${}^{14}_{4}Be_{10}$ focusing on the problem of N=8 magicity. We will also study a proton-drip line nucleus ${}^{13}_{8}O_5$ to find out a possible melting of shell gap at Z=8 in nuclei near the proton drip line. As the theoretical framework, we adopt a large scale shell model including $(0+2)\hbar\omega$ model space for the ground states and $(1+3)\hbar\omega$ model space for the excited states. In section 2, we describe the model. Calculated results are shown in section 3. Section 4 is devoted to discussions. Conclusions are given in section 5.

II. MODEL

In this study, we adopt the following large model space in the shell model calculations. The effects of higher configurations are taken into account up to $2\hbar\omega$ excitations for the ground states and up to $3\hbar\omega$ excitations for the excited states. Millener-Kurath interaction PSDMK2 [20] and Warburton-Brown interaction WBP [21] are used as the effective interactions for the (1p-2s1d) model space and for (1s-1p-2s1d-1f2p) model space, respec-

tively. It is shown that these interactions can explain well the spectra and the ground state properties of most of the neighboring A=5−16 nuclei by PSDMK2 [20,22] and A=10−22 nuclei by WBP interaction. For PSDMK2 interaction, the single particle energy of the $2s_{1/2}$ orbit is lowered to admix sd-shell components in the ground state as suggested by recent analysis of G-T strength [19] and the Coulomb energy in $^{11}_{3}Li_8$ [23]. We name this interaction PSDMK2*. The probability of the p-shell components is claimed to be 45 $\sim$ 55 % in these study. The adopted value of the p-state probability in this study is 46.2 % in $^{11}_{3}Li_8$. Extended wave functions are used for the neutron (or proton) $1p_{1/2}$ and $2s_{1/2}$ orbits in $^{12}_{4}Be_8$ and $^{14}_{4}Be_{10}$ ($^{13}_{8}O_5$). Their radial wave functions are calculated based on the Hartree-Fock (HF) potential with SGII interaction. The obtained HF central potential depth of each nucleus is adjusted by multiplying a scaling factor to reproduce the half of the empirical two neutron (proton) separation energies S_{2n}=3.67 MeV for $^{12}_{4}Be_8$ and S_{2n}=1.34 MeV for $^{14}_{4}Be_{10}$, respectively (S_{2p}=2.12 MeV for $^{13}_{8}O_5$). A similar prescription for the extended wave functions is successfully used in the study of low energy dipole and GT transitions in $^{11}_{3}Li_8$ [16,19].

The center of mass spurious components in the wave functions are pushed up to higher excitation energies by adding a fictitious hamiltonian which acts only on the center of mass excitation [24]. This procedure, so called Lawson method, will remove almost 100% of the spurious components in the wave functions when we adopt the harmonic oscillator basis. In the present case of modified HF wave functions, small spurious components still remain in the shell model wave functions. We use the effective E1 transition operator to remove further these spurious components,

$$\hat{O}^{\lambda=1}_{\mu} = e\frac{Z}{A}\sum_{i}^{N} r_i Y_{1\mu}(\hat{r}_i) - e\frac{N}{A}\sum_{i}^{Z} r_i Y_{1\mu}(\hat{r}_i) \tag{1}$$

in which the spurious center-of-mass motion is subtracted from the isovector dipole transition operator. The E1 transition strength to n-th excited state at energy E_n is defined as

$$B(E1, E_n) = \frac{1}{2J_i+1}\sum_{M_i,\mu,M_f} \mid \langle n; J_f, M_f \mid \hat{O}^{\lambda=1}_{\mu} \mid J_i, M_i \rangle \mid^2 . \tag{2}$$

The transition strength is averaged by a weight factor $\rho(\omega)$ as

$$\frac{dB(E1;\omega)}{d\omega} = \sum_n B(E1;\omega_n)\rho(\omega-\omega_n) \tag{3}$$

where

$$\rho(\omega-\omega_n) = \frac{1}{\pi}\frac{\Gamma/2}{(\omega-\omega_n)^2+(\Gamma/2)^2}. \tag{4}$$

The weight factor can be considered to simulate the escape and the spreading widths.

The sum rule is an useful measure of the collectivity in giant resonances (GR). For the isovector (IV) GDR, the energy weighted sum rule value is given by

$$S(TRK) = \sum_n |< n|\hat{O}_\mu^{\lambda=1}|gs>|^2 = \frac{\hbar^2}{2m}\frac{9}{4\pi}\frac{NZ}{A}e^2 = 14.9\frac{NZ}{A}e^2 \ \text{(MeV·fm}^2\text{)} \tag{5}$$

neglecting the contributions of exchange terms. This sum rule is known as the classical Thomas-Reiche-Kuhn (TRK) sum rule. The photoreaction cross section σ_{int} is then expressed as [25]

$$\sigma_{int} = \frac{16\pi^3}{9\hbar c}S(TRK) = 60\frac{NZ}{A} \ \text{(MeV·mb)}. \tag{6}$$

The cluster sum rule is referred often to measure the adiabaticity between GDR and Pigmy resonance [6]. Assuming the valence cluster with N_2 and Z_2 and the core with N_1 and Z_1, the cluster sum rule is given by

$$S(\text{cluster}) = \frac{\hbar^2}{2m}\frac{9}{4\pi}\frac{(Z_1A_2 - Z_2A_1)^2}{AA_1A_2} \tag{7}$$

where $A_1 = N_1 + Z_1$ and $A_2 = N_2 + Z_2$.

III. NUMERICAL RESULTS

In Figs. 1, 2 and 3, we show the results of two calculations of the dipole transitions in $^{12}_{4}\text{Be}_8$, $^{14}_{4}\text{Be}_{10}$ and $^{13}_{8}\text{O}_5$ with the extended single particle wave functions and with the harmonic oscillator wave functions, respectively. The size parameter for the harmonic oscillator is taken to be a standard value b=1.64 fm, which corresponds to $\hbar\omega = 15.7$ MeV. The width parameter Γ in Eq. (4) is taken to be 0.5MeV.

A. Dipole strength in $^{12}_{4}Be_8$

In Fig. 1(a), we show two calculated results of the dipole transitions in $^{12}_{4}Be_8$ by PSDMK2* with the extended single particle wave functions and with the harmonic oscillator wave functions. We can see from Fig. 1(a) that substantial strength appears at E_x =2.36MeV far below the GDR region at $E_x = 10 \sim 13$ MeV, only when the effect of the extended single particle wave functions is switched on. On the other hand, the GDR peaks are found above E_x =10MeV and not so much affected by the effect of the extended single particle wave functions. The low energy transition strength is found to be B(E1)=0.063 e^2fm^2 at E_x =2.36MeV. This B(E1) value corresponds to 0.19 Weisskopf unit (W.u.) and amounts to 0.4% of the TRK sum rule value (5) and 4.0% of the cluster sum rule value (7). The calculated value shows good agreement with the observed value B(E1)=0.051(13) e^2fm^2 at E_x = 2.68(3) MeV by recent Coulomb excitation experiments [5]. This E1 strength corresponds to the second largest E1 strength among the transitions between bound states, next to the transition between $1/2^+$ and $1/2^-$ states in$^{11}_{4}Be_7$ with B(E1)=0.36±0.03 W.u. . The integrated transition strength of GDR in the energy regions E_x=(10−15), (15−20) and (20−30)MeV exhaust 15.7%, 12.7% and 15.5% of the TRK sum rule.

We have done also more elaborate shell model calculations including the 1f2p shell configurations in addition to the 1p-2s1d shells with a Warburton-Brown interaction, WBP [21]. The first 1^- peak is found at E_x=2.90MeV, having B(E1)=0.072 e^2fm^2. These values are surprisingly close to those of PSDMK2* interaction, although both the model space and the effective interaction are different. Generally speaking, the structure of GDR above E_x=10MeV is similar in the two results. However, in the case of WBP interaction, larger E1 strength are found in the energy regions $E_x = (5 - 10)$MeV and $(20 - 30)$MeV, while there are not so much strength in the same regions in the case of PSDMK2*. The B(E1) strength of WBP interaction exhausts 9.6%, 16.0%, 7.2%, and 64% of the TRK sum rule in the energy regions $E_x = (5 - 10), (10 - 15), (15 - 20)$ and $(20 - 30)$MeV , respectively. The larger value in the region $E_x = (20 - 30)$MeV in comparison with PSDMK2* case is due to

the larger model space including (1f2p) shell for the WBP interaction.

The large E1 strength in the very low energy region below E_x=3MeV can be considered due to a coherence in the oscillation between the loosely-bound neutrons, and also between the core and the loosely-bound neutrons. The low energy vibration mode in nuclei with loosely-bound neutrons was originally suggested by Ikeda [26], and Hansen and Jonson [27] independently and called "soft dipole mode". Their conjectures are somewhat different each other and also different to the present idea of the low energy vibration mode. In order to clarify the mechanism of the enhancement, we discuss the low energy dipole state as a doorway state of the correlated ground state [5,16]. Firstly, the $^{12}_{4}$Be$_8$ ground state is described to be a state of correlated two neutrons in $(1p_{1/2})^2$ and $(2s_{1/2})^2$ states moving outside of ^{10}Be core,

$$|^{12}_{4}\mathrm{Be}_8 : 0^+ >= \alpha|(1p_{1/2})^2 > +\beta|(2s_{1/2})^2 > . \tag{8}$$

In the limit of the complete degeneracy of the two orbitals, we have the amplitudes $\alpha = \beta = \frac{1}{\sqrt{2}}$. Then a coherent 1^- excitation of the correlated two neutrons is written as a doorway state for the dipole operator (1),

$$\begin{aligned} |^{12}_{4}\mathrm{Be}_8 : 1^- > &= \frac{1}{\sqrt{N}}\hat{O}^{\lambda=1}|^{12}_{4}\mathrm{Be}_8 : 0^+ > \\ &= 0.63|(2s_{1/2}1p^{-1}_{1/2}) > +0.63|(1p_{1/2}2s^{-1}_{1/2}) > +0.45|(2s_{1/2}1p^{-1}_{3/2}) >, \end{aligned} \tag{9}$$

where N is a normalization constant, and the coefficients are proportional to the single particle matrix elements of the dipole operator $\hat{O}^{\lambda=1}$. In Eq. (9), the particle-hole excitations are limited to the configuration space of $1p$ and $2s$ orbitals to pin down specifically the coherence in the loosely-bound neutron configurations. The coefficients of the p-h configurations are obtained taking into account the effect of small separation energies of the $1p_{1/2}$ and $2s_{1/2}$ states in $^{12}_{4}$Be$_8$. The B(E1) value between the two states (8) and (9) is expressed as

$$\begin{aligned} B(\mathrm{E1}; 0^+ \to 1^-) &= | < 1^-||\hat{O}^{\lambda=1}||0^+ > |^2 \\ &= |0.63 < 2s_{1/2}||\hat{O}^{\lambda=1}||1p_{1/2} > \\ &+ 0.63 < 1p_{1/2}||\hat{O}^{\lambda=1}||2s_{1/2} > +0.45 < 2s_{1/2}||\hat{O}^{\lambda=1}||1p_{3/2} > |^2. \end{aligned} \tag{10}$$

We can see in Eq. (10) that the degeneracy of $1p_{1/2}$ and $2s_{1/2}$ states indeed enhances the B(E1) value more than twice of the single-particle transition rate between $1p_{1/2}$ and $2s_{1/2}$ states. For more quantitative study of the dipole states in $^{12}_{4}$Be$_8$, we have to take into account the excitations of core neutrons to the higher orbits than the loosely-bound configurations. Especially, the $(1p_{3/2} \rightarrow 1d_{5/2})$ excitation has an important contribution to the E1 transition.

The two-neutron pairing model is used to describe 1^- states in $^{12}_{4}$Be$_8$ recently by Bonaccorso and N. Vinh Mau [28]. Their results predicted the lowest 1^- state in $^{12}_{4}$Be$_8$ at 2.7 MeV with a larger B(E1) value of 0.23 e^{2}fm^2 than the present results. They also pointed out that the strong correlation between the $(1p_{1/2})^2$ and $(2s_{1/2})^2$ configurations enhances the E1 strength. The difference of the calculated B(E1) value from the present shell model results might be attributed to that of extended neutron wave functions adopted in ref. [28] where the one neutron separation energy of $^{11}_{4}$Be$_7$, S$_{1n}$=0.5MeV, is used for the renormalization of the Woods-Saxon potential.

B. Dipole strength in $^{14}_{4}$Be$_{10}$

Results of two calculations in $^{14}_{4}$Be$_{10}$ with the extended single particle wave functions and with the harmonic oscillator wave functions are shown in Figs. 2(a) and 2(b) using PSDMK2* and WBP interaction, respectively. Compared with the results of $^{12}_{4}$Be$_8$ in Fig. 1, it is remarkable that there is no E1 strength below 5MeV in Fig. 2. Two peaks appear in the energy region between E$_x$=(5−10)MeV of Fig. 2(a), i.e., a peak at E$_x$=7.35MeV with B(E1)=0.097 e^{2}fm^2 and another peak at E$_x$=9.86MeV with B(E1)= 0.119 e^{2}fm^2 when the effect of the extended single particle wave functions is switched on. These two peaks exhaust 4.4% of the TRK sum rule (5) and 27.8% of the cluster sum rule (7). It is interesting to notice that the effect of the extended single particle wave functions increases the B(E1) strength at E$_x$=7.35MeV by about 60% , while the increase of the low energy strength in $^{12}_{4}$Be$_8$ is 60 times more than the value with the harmonic oscillator wave functions. The main GR peak appears in the energy region E$_x$=(11 −15)MeV and substantial strength can be

seen also above E_x= 16MeV. The E1 strength between E_x=(11 −20)MeV exhausts 33.9% of the TRK sum rule. While a clear difference can be seen in the excitation energies of the low energy E1 strength between $^{12}_{4}Be_8$ and $^{14}_{4}Be_{10}$, the energies of GDR remain at almost the same energy region. We will discuss the relation between the excitation energy of the low energy E1 strength and the shell gap in detail in section 4.

The results of WBP interaction are shown in Fig. 2(b). The lowest E1 peak is found at E_x=7.46MeV with B(E1)=0.110 e^2fm^2 when the effect of the extended single particle wave functions is taken into account. Two results in Figs. 2(a) and 2(b) are very consistent to predict the lowest 1^- state both for the excitation energy and the B(E1) strength. The GDR peaks above 10MeV are more pronounced and more spread in Fig. 2(b). This result is entirely due to the larger model space of WBP interaction, which might be important to predict the GDR strength properly. The B(E1) values in the energy region E_x=(10-15), (15-20) and (20-30)MeV exhaust 13.2%, 40.0% and 43.6% of the TRK sum rule, respectively in the case with the effect of the extended single particle wave functions. There are not so much difference in the two curves in Fig. 2(b) as far as the E1 strength above 10MeV are concerned.

C. Dipole strength in $^{13}_{8}O_5$

In Figs. 3(a) and 3(b), the calculated results of E1 strength in $^{13}_{8}O_5$ are shown with the WBP interaction. In Fig. 3(a), the E1 strength from the ground state J^π=3/2$^-$ to the excited states J^π=1/2$^+$, 3/2$^+$ and 5/2$^+$ are drawn by the solid, dashed and dashed-dotted curves, respectively, with the effect of the extended single particle wave functions. The summed E1 strength of all the final states are given in Fig. 3(b) with the extended single particle wave functions and with the harmonic oscillator wave functions by the solid and dashed curves, respectively. The enhancement of the low energy strength in $^{13}_{8}O_5$ appears mainly in the three states at E_x = 2.92 MeV (1/2$^+$), 5.76 MeV (5/2$^+$) and 6.25 MeV (3/2$^+$) as shown in Figs. 3(a) and (b). For these three states, the proton particle-hole transitions,

$(\pi 1p_{1/2} \rightarrow \pi 2s_{1/2})$, $(\pi 2s_{1/2} \rightarrow \pi 1p_{1/2})$ and $(\pi 1p_{3/2} \rightarrow \pi 2s_{1/2})$ transitions, contribute coherently to enhance the strength. The former two configurations are due to the excitations of the center of mass of the two loosely-bound configurations $(\pi 2s_{1/2})^2$ and $(\pi 1p_{1/2})^2$, while the last one is the excitation of the core particle to the loosely-bound orbit. This microscopic structure of the wave functions suggests a coherent excitation between the loosely-bound protons, and also between the core and the loosely-bound protons, similar to the excitations in the nuclei with loosely-bound neutrons $^{11}_{3}\mathrm{Li}_8$ and $^{12}_{4}\mathrm{Be}_8$. Then this coherent excitation couples with the neutron hole configuration $(\nu 1p_{3/2})^{-1}$ and splits the B(E1) strength to the three low excited states, while the proton particle $(\pi 1p_{3/2})$ state couples with the neutron vibrational state in $^{11}_{3}\mathrm{Li}_8$.

We now introduce the particle-vibration coupling model to understand the microscopic structure of the splitting of low energy dipole excitations in $^{13}_{8}\mathrm{O}_5$. Since the three valence neutrons in the $1p_{3/2}$-shell can make only the configuration of seniority 1, it is convenient to adopt the hole picture, instead of the particle one which was adequate for $^{11}_{3}\mathrm{Li}_8$. The hole-vibration coupling gives the same intensity rule for the transition strength as that of the particle-vibration coupling, but the energy splitting will be changed in the opposite direction. The B(E1) values for the coupled states are related to the B(E1) value of the 1^-−phonon excitation in the core as [29]

$$B(E1; 3/2^- \rightarrow (1^- \times 3/2^-)J) = \frac{2J+1}{3 \cdot 4} B(E1; 0^+ \rightarrow 1^-). \tag{11}$$

The B(E1; $0^+ \rightarrow 1^-$) value can be deduced from the sum of the three transition strength 0.056, 0.053 and $0.114 e^2 fm^2$ to the states with the $J^\pi = 1/2^+$, $3/2^+$ and $5/2^+$, respectively, and is calculated to be $0.223\ e^2 fm^2$. This is close to the B(E1) value for the ideal phonon which is calculated to be $0.171\ e^2\mathrm{fm}^2$ in $^{14}\mathrm{O}$. We can see that the ratio of transition strength to the low energy dipole states with spin J is approximately 1:1:2, which does not obey the $2J+1$ rule strictly. This is due to the fact that the admixture of the $(\nu 1p_{3/2}^2 1p_{1/2})$ configurations are not small in the excited states and the assumption of the pure $(\nu 1p_{3/2}^3)$ configuration is broken to a certain amount.

The particle-vibration coupling model can be also applied to calculate the energy splitting of the low energy dipole states. Assuming an interaction of the separable form $(Y^{(2)} \times Y^{(2)})^{(0)}$ for the hole-phonon coupling, the energy shift of the low energy dipole state with spin J is given by

$$\langle (1p3/2)^{-1} \times (1^-); J \mid H \mid (1p3/2)^{-1} \times (1^-); J \rangle = \omega_{1^-} + \begin{cases} -5c_2, & for \quad J = 1/2^+ \\ 4c_2, & for \quad J = 3/2^+ \\ -c_2, & for \quad J = 5/2^+ \end{cases} \qquad (12)$$

where ω_{1^-} is the 1^--phonon energy and c_2 comes from the quadrupole interaction. We should notice that the sign of the particle-vibration matrix element has the opposite sign between the particle and the hole in the same orbit. Therefore the $J=1/2^+$ state is the lowest in the energy in$^{13}_{8}O_5$, while the $J=3/2^+$ state is the lowest in $^{11}_{3}Li_8$. We obtain ω_{1^-} = 5.45 MeV by taking an weighted average over the energies, E_J, of the low energy dipole states; $(2\times E_{1/2} + 4\times E_{3/2} + 6\times E_{5/2})/12$ with $E_{1/2}$ = 2.92 MeV, $E_{3/2}$ = 6.25 MeV and $E_{5/2}$ = 5.76 MeV. The coefficient c_2 is determined to be 0.506 MeV from comparison to the energy of $1/2^+$ state. The value of ω_{1^-} = 5.45 MeV is close to the excitation energy of the 1^- state in $^{14}_{8}O_6$. Although the ordering of the energies of the low energy dipole states is correctly predicted, the positions of $3/2^+$ and $5/2^+$ states are not very well reproduced by eq. (12) when c_2 value determined above is used. This can be also attributed to the mixing of $(\nu 1p^2_{3/2} 1p_{1/2})$ configurations.

In the present shell model calculations, the energy levels of the mirror nuclei $^{13}_{5}B_8$ are predicted to be the same as those of $^{13}_{8}O_5$. Experimentally , the lowest excited levels are observed in $^{13}_{5}B_8$ at around E_x=3.5MeV, while the spins and the parities of these levels are not yet assigned. According to the present shell model results, the spin of the lowest positive parity state is also most probably $J=1/2^+$ in $^{13}_{5}B_8$ having somewhat higher energy than that in $^{13}_{8}O_5$. Recently, the Coulomb dissociation cross sections of $^{13}_{8}O_5$ was measured at RIKEN [30]. They claim large E1 strength in the same low energy region as the present calculated results.

IV. DISCUSSIONS

The location of the lowest 1^- state in p-shell nuclei may provide a critical measure of the energy difference between the $1p_{1/2}$ and (1d2s) shell orbitals, since the dominant configurations of the lowest 1^- state are expected to be the excitations $(1p_{1/2} \rightarrow 2s_{1/2})$ and $(1p_{3/2} \rightarrow 1d_{5/2}, 2s_{1/2})$ from the naive shell model picture. When a nucleus locates closer to the drip line, the Fermi energy becomes smaller and eventually goes to zero at the drip line. Consequently, the sd shell orbits are close to the threshold in neutron-rich Be-isotopes. In very neutron-rich nuclei, the single particle energy of $2s_{1/2}$ state becomes lower than that of $1d_{5/2}$ state because of more pronounced effect of the loosely-binding on the lower angular momentum state, as shown by the mean field calculations [31,12,32]. Thus the systematic study of the excitation energies of the 1^- states (equivalently the energies of the lowest E1 transitions) of Z=4 isotopes or Z=8 isotopes may clarify the change of the energy difference between $1p_{1/2}$ and $2s_{1/2}$ states.

Fig. 4 shows the positive and negative parity states of Be- and O-isotopes involved in the lowest E1 transitions. In $^{11}_{4}Be_7$, the negative J=1/2$^-$ state is almost degenerate near the ground state with J=1/2$^+$ and a strong E1 transition between the two states is observed [4]. The 1^- state appears also at a very low energy E_x=2.68MeV in $^{12}_{4}Be_8$. They manifest a clear sign of the melting of energy gap between p- and sd-shells in the nuclei near the neutron drip line. The excitation energy of the lowest 1^- state appears rather high energy in $^{14}_{4}Be_{10}$ in the present calculations. This is because both the almost degenerate $1p_{1/2}$ and $2s_{1/2}$ orbits are filled up in $^{14}_{4}Be_{10}$, and available p-h configurations (for example, $1p_{3/2} \rightarrow 1d_{5/2}$) will be rather high in the excitation energy. We can see in Fig. 4 that the predicted excitation energy of the lowest 1^- state in $^{14}_{4}Be_{10}$ is very close to the observed one E_x=7.12MeV of the lowest 1^- state in the doubly closed shell nucleus $^{16}_{8}O_8$.

In O-isotopes, the lowest E1 transition partners are 7.12MeV in $^{16}_{8}O_8$, 5.18MeV in $^{15}_{8}O_7$ and 5.11MeV in $^{14}_{8}O_6$ as shown in Fig. 4(b). The energy difference drops sharply in $^{13}_{8}O_5$ to E_x=2.92MeV according to the present calculations. This trend looks similar to the finding

in the E1 partners of Be-isotopes in Fig. 4(a). Further experimental study is highly desired for the low energy 1^- states both in $^{14}_{4}Be_{10}$ and $^{13}_{8}O_5$ to establish a possible large shell gap at N=10, and also the melting the proton shell gap at Z=8.

There is a conjecture [26,27] that a vibration between the loosely-bound neutrons and the core will create a low excited collective state far below GDR energy region. On the other hand, it was shown that the quantum mechanical effect enhances enormously the transition strength from the loosely bound nucleons to the continuum near the threshold in halo nuclei [33,34]. This threshold effect explains the energy dependence and the absolute magnitude of the observed low energy dipole strength in the halo nucleus $^{11}_{4}Be_7$. There are significant differences in the structure of loosely-bound nucleons between $^{11}_{4}Be_7$, $^{12}_{4}Be_8$ and $^{13}_{8}O_5$, and also between $^{11}_{4}Be_7$ and $^{11}_{3}Li_8$. Namely one neutron halo configuration exists for $^{11}_{4}Be_7$, while two neutron or two proton extended wave functions might be correlated in the cases of $^{12}_{4}Be_8$, $^{13}_{8}O_5$ and $^{11}_{3}Li_8$. Furthermore, the separation energy may not be small enough to make "halo" in $^{12}_{4}Be_8$ and $^{13}_{8}O_5$, while the two loosely-bound neutrons in $^{11}_{3}Li_8$ have a very small two neutron separation energy S_{2n}=320keV and are confirmed experimentally to have the "halo" structure [1]. Irrespective of these differences, we see the large E1 strength induced by the coherence in the dipole configurations with $1p_{1/2}$ and $2s_{1/2}$ orbits, in the very low energy region of all the nuclei above mentioned. It would be an interesting question to confirm experimentally how much extent the coherent vibration picture between the loosely-bound nucleons and the core is appropriate to explain the large dipole strength in these nuclei. In this respect, $^{12}_{4}Be_8$ is an ideal case to check the idea of the coherent excitation since the B(E1) strength appears below the threshold. The good agreement of the present calculations and the experimental observations both in the excitation energy and the B(E1) strength can be considered as empirical evidence of the coherent effect on the low energy dipole state in $^{12}_{4}Be_8$.

V. CONCLUSIONS

We have studied electric dipole transition strength in the three nuclei with loosely-bound nucleons $^{12}_{4}Be_8$, $^{14}_{4}Be_{10}$ and $^{13}_{8}O_5$ by the large scale shell model calculations including the configuration space up to $3\hbar\omega$ excitations. We found large low energy E1 peaks at E_x=2.36MeV in $^{12}_{4}Be_8$ and E_x=2.92MeV in $^{13}_{8}O_5$, having the E1 strength B(E1)=0.063 and 0.056 e^2fm^2, respectively. The calculated results in $^{12}_{4}Be_8$ show good agreement with the recently observed 1^- state at E_x = 2.68(3) MeV with B(E1)=0.051(13) e^2fm^2 by the Coulomb excitation. In $^{14}_{4}Be_{10}$, the lowest 1^- state is predicted at E_x=7.46MeV which is much higher than the energy in $^{12}_{4}Be_8$. This large difference is due to the fact that the almost degenerate $1p_{1/2}$-$2s_{1/2}$ orbits are filled up in $^{14}_{4}Be_{10}$ and the available p−h configurations are much higher in energy than that of $^{12}_{4}Be_8$. The E1 strength is predicted also at a low energy E_x=2.92MeV in the proton drip line nucleus $^{13}_{8}O_5$, while the E1 partners have the energy difference 5.18MeV in $^{15}_{8}O_7$. The low energy E1 strength in $^{12}_{4}Be_8$ and $^{13}_{8}O_5$ can be interpreted as the sign of the melting of the energy gaps at N=8 and Z=8 near the drip lines. Furthermore the high excitation energy of the lowest 1^- state in $^{14}_{4}Be_{10}$ suggests a large shell gap at N = 10 near the neutron drip line . We pointed out two key issues to obtain the extremely enhanced E1 strength at the low energy. The first one is the effect of the extended wave functions, which enlarges the single particle transition matrix elements, and also induces the decoupling of the enhanced low energy E1 strength from the GDR strength. The second one is the coherence in the transition amplitudes between the loosely-bound nucleons, and also between the core and the loosely-bound nucleons. The hole-vibration coupling picture is used to interpret the splittings of both the energies and the strength in $^{13}_{8}O_5$. Further experimental and theoretical efforts are desperately needed for solid establishment of the new coherent effect on the E1 transitions and a large shell gap at N=10 near the drip lines.

The authors are grateful to Prof. T. Motobayashi for drawing their attention to the E1 strength in $^{13}_{8}O_5$ and for enlightening discussions. This work is supported in part by the Ministry of Education, Science, Sports and Culture by Grant-In-Aid for Scientific Research

under the program numbers (C(2)) 12640284 and (B) 08454069.

REFERENCES

[1] I. Tanihata et al., Phys. Lett. **B287** (1992) 307, and references therein;
I. Tanihata, J. Phys. **G22**, 157 (1996).

[2] P. G. Hansen, A. S. Jensen and B. Jonson, Ann. Rev. Nucl. Part. Sci. **45**, 591 (1995).

[3] T. Kobayashi, in *Proceedings of the International Symposium on Structure and Reactions of Unstable Nuclei*, Niigata, 1991, ed. by K. Ikeda and Y. Suzuki (World Scientific, Singapore, 1991), p.187.

[4] D. J. Millener *et al.*, Phys. Rev. **C28** , 497 (1983).

[5] H. Iwasaki *et al.*, Riken preprint (RIKEN-AF-NP-357).

[6] H. Sagawa and M. Honma, Phys. Lett.**B251**, 17 (1990).

[7] K. Ieki *et al.*, Phys. Rev. Lett. **70**, 730 (1993); D. Sackett *et al.*, Phys. Rev. **C48**, 118 (1993).

[8] S. Shimoura, T. Nakamura, M. Ishihara, N. Inabe, T. Kobayashi, T. Kubo, R. H. Siemssen, I. Tanihata and Y. Watanabe, Phys. Lett. **B348**, 29 (1995).

[9] M. Zinser et al., Nucl. Phys. **A619**, 151 (1997).

[10] T. Nakamura *et al.*, Phys. Lett. **B331**, 296 (1994).

[11] A. Navin *et al.*, Phys. Rev. Lett. **85**, 266 (2000).

[12] A. Ozawa *et al.*, Phys. Rev. Lett. **84**, 5493 (2000).

[13] H. Iwasaki *et al.*, Phys. Lett. **B 481**, 7 (2000).

[14] T. Motobayashi et al., Phys. Lett.**B 346**, 9 (1995).

[15] C. Détraz *et al.*, Phys. Rev. **C 19**, 164 (1979);
D. Guillemaud-Mueller *et al.*, Nucl. Phys. **A 426**, 37 (1984).

[16] Toshio Suzuki, H. Sagawa and P. F. Bortignon, Nucl. Phys. **A 662**, 282 (2000).

[17] N. Aoi et al., Nucl. Phys. **A616**, 181c (1997); Z. Phys. **A358**, 253 (1997).

[18] M. J. Borge et al., Phys. Rev. **C55**, R8 (1997).
E. Roeckel, D. F. Dittner, C. Détraz, R. Klapisch, C. Thibault and C. Rigaud, Phys. Rev. **C10**, 1181 (1974).

[19] T. Suzuki and T. Otsuka, Phys. Rev. **C56**, 847 (1997); **C50**, R555 (1994).

[20] D. J. Millener and D. Kurath, Nucl. Phys. **A255**,315 (1975).

[21] E. K. Warburton and B. A. Brown, Phys. Rev. **C46**, 923 (1992) and private communications.

[22] S. Cohen and D. Kurath, Nucl. Phys. **73**, 1 (1965).

[23] T. Suzuki and T. Otsuka, Nucl. Phys. **A635**, 86 (1998).

[24] D. H. Gloeckner and R. D. Lawson, Phys. Lett. **B53**, 313 (1974).

[25] A. Bohr and B. R. Mottelson, *Nuclear Structure Vol. II* (Benjamin, New York, 1975) p.478.

[26] K. Ikeda et al., Nucl. Phys. **A538**, 355c (1992).

[27] P. G. Hansen and B. Jonson, Europhys. Lett. **4**, 409 (1987).

[28] A. Bonaccorso and N. Vinh Mau, Nucl. Phys. **A 615**, 245 (1997).

[29] p.571 and p.360 in ref. [25].

[30] T. Minemura et al., Riken Accelerator Progress Report **33**, 63 (2000).

[31] H. Sagawa, B. A. Brown and H. Esbensen, Phys. Lett. **B309**, 1 (1993).

[32] I. Hamamoto, S. V. Lukyanov and X. Z. Zhang, preprint (2000).

[33] H. Sagawa, Nguyen Van Giai, N. Takigawa, M. Ishihara and K. Yazaki, Z. Phys. **A351**,

385 (1995).

F.Catara, C. H. Dasso and A.Vitturi, Nucl. Phys. **A602**, 181 (1996).

[34] S. Karataglidis, P. G. Hansen, B. A. Brown, K. Amos and P. J. Dortmans, Phys. Rev. Lett **79**, 1447 (1997).

FIGURES

FIG. 1. Calculated results of E1 strength distribution (3) in $^{12}_{4}Be_{8}$. The solid curve shows the result with the effect of the extended single particle wave functions , while the dashed one corresponds to that with the harmonic oscillator wave functions: a) PSDMK2* interaction, b) WBP interaction.

FIG. 2. Calculated results of E1 strength distribution (3) in $^{14}_{4}Be_{10}$. The solid curve shows the result with the effect of the extended single particle wave functions , while the dashed one corresponds to that with the harmonic oscillator wave functions: a) PSDMK2* interaction, b) WBP interaction.

FIG. 3. Calculated results of E1 strength distribution (3) in $^{13}_{8}O_{5}$ with WBP interaction; (a) the solid, dashed and dotted-dashed curves show the E1 strength to $J^{\pi}=1/2^{+}$, $3/2^{+}$ and $5/2^{+}$ states, respectively, with the effect of the extended single particle wave functions. (b) the summed E1 strength distribution of the all spin states. The solid curve shows the result with the effect of the extended single particle wave functions , while the dashed one corresponds to that with the harmonic oscillator wave functions.

FIG. 4. Energy levels in the Be- and O- isotopes. Experimental values are shown by solid lines, while calculated values are shown by dashed lines.

Figure 1

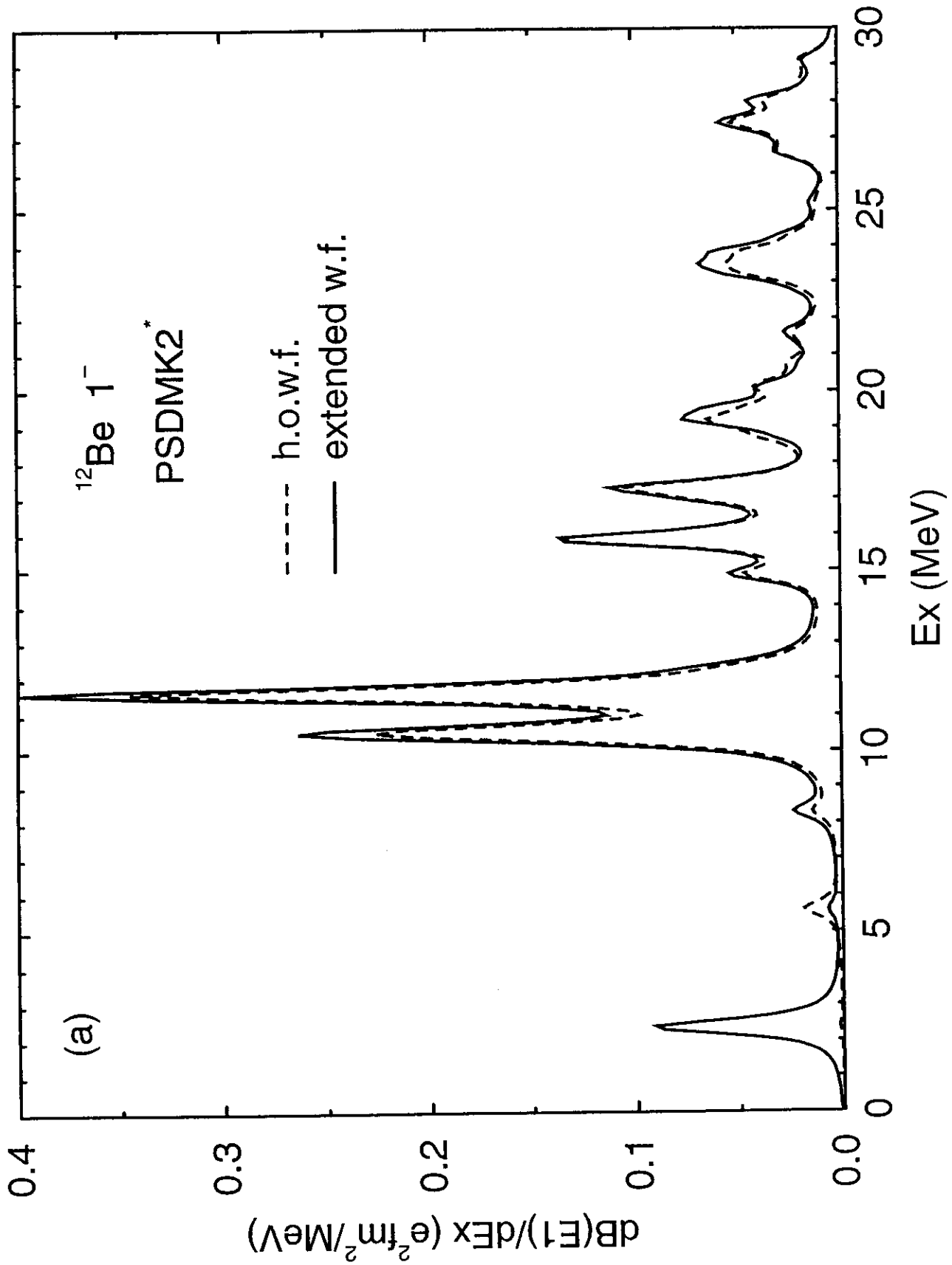
(a)
^{12}Be 1$^-$
PSDMK2*
h.o.w.f.
extended w.f.
dB(E1)/dEx (e^{2}fm^2/MeV)
Ex (MeV)
0.0
0.1
0.2
0.3
0.4
0
5
10
15
20
25
30

Figure 1

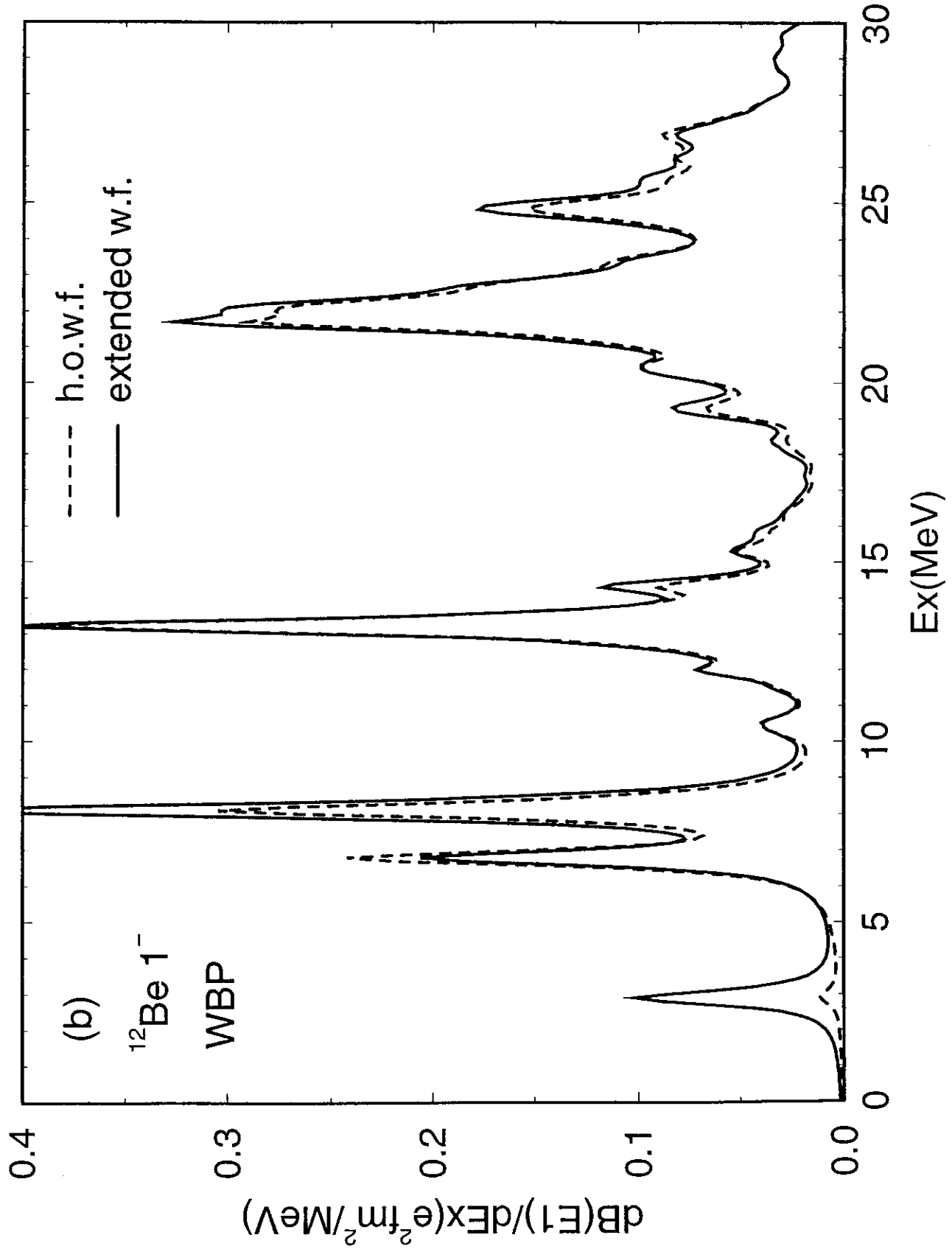
(b)
^{12}Be 1$^-$
WBP
h.o.w.f.
extended w.f.
dB(E1)/dEx(e^{2}fm^2/MeV)
Ex(MeV)
0.0
0.1
0.2
0.3
0.4
0
5
10
15
20
25
30

Figure 2

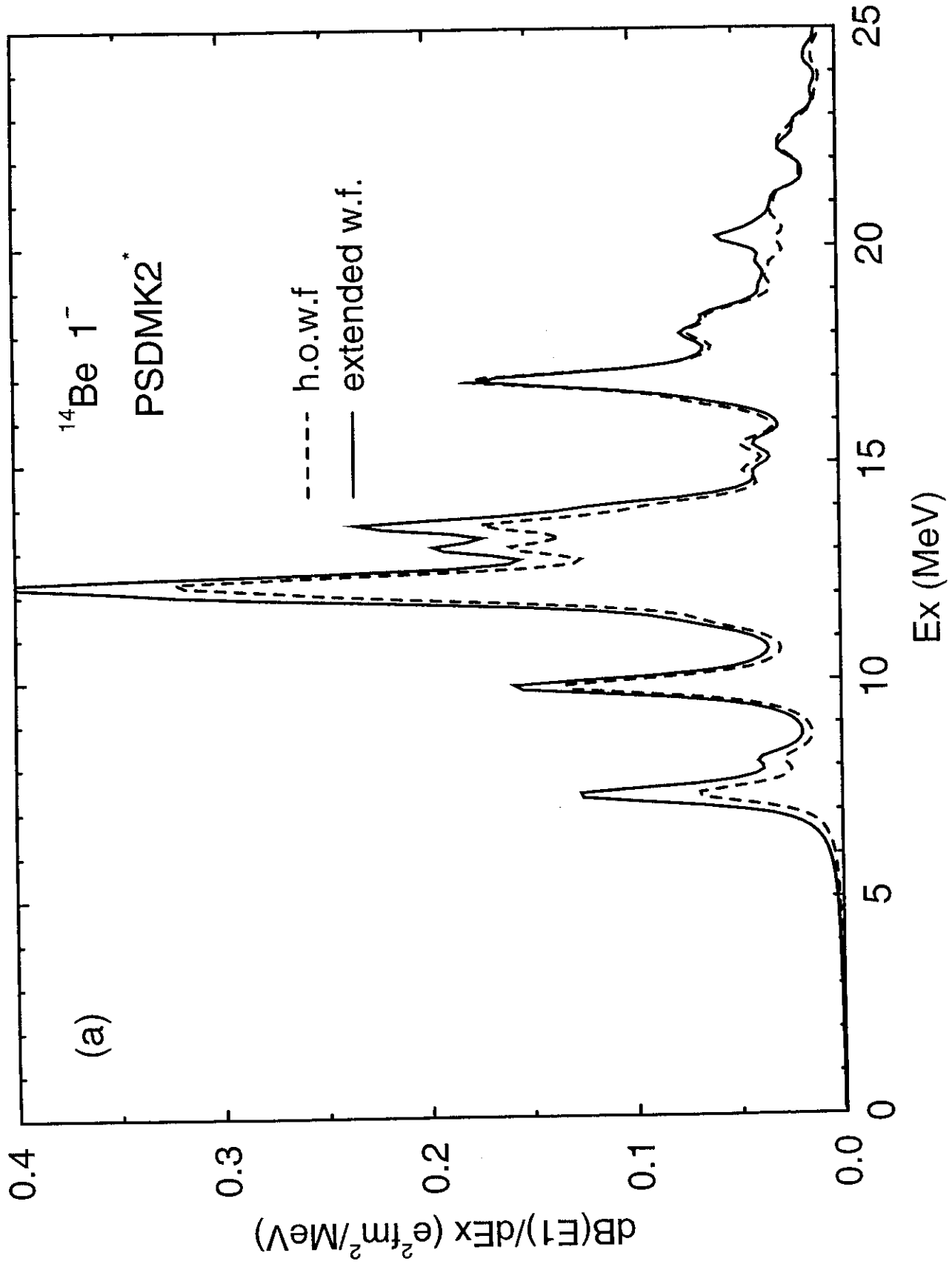
(a)
^{14}Be 1$^-$
PSDMK2*
h.o.w.f
extended w.f.
dB(E1)/dEx (e^{2}fm^2/MeV)
Ex (MeV)
0.0
0.1
0.2
0.3
0.4
0
5
10
15
20
25

Figure 2

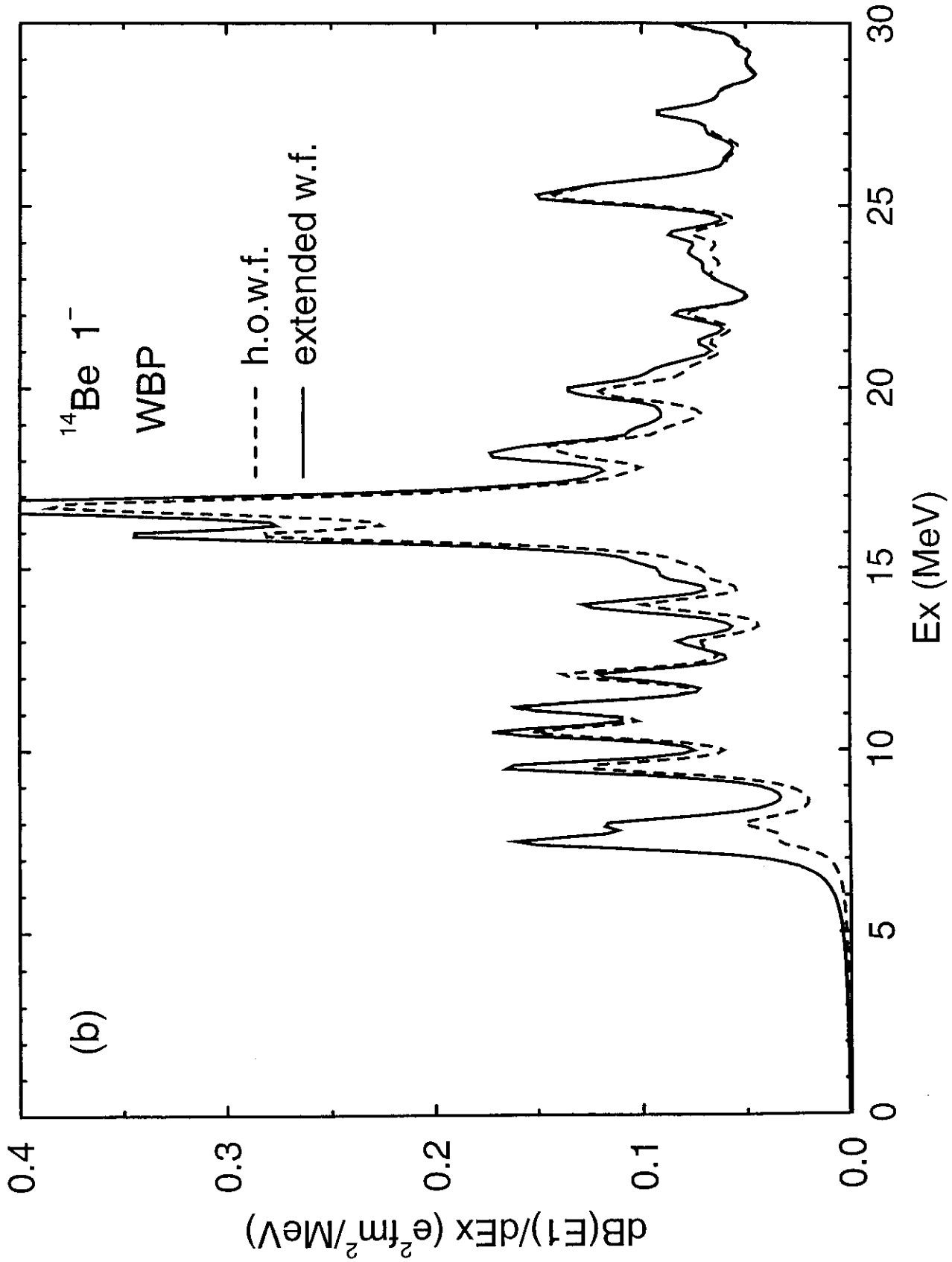
(b)
^{14}Be 1$^-$
WBP
h.o.w.f.
extended w.f.
dB(E1)/dEx (e^{2}fm^2/MeV)
Ex (MeV)
0.0
0.1
0.2
0.3
0.4
0
5
10
15
20
25
30

Figure 3

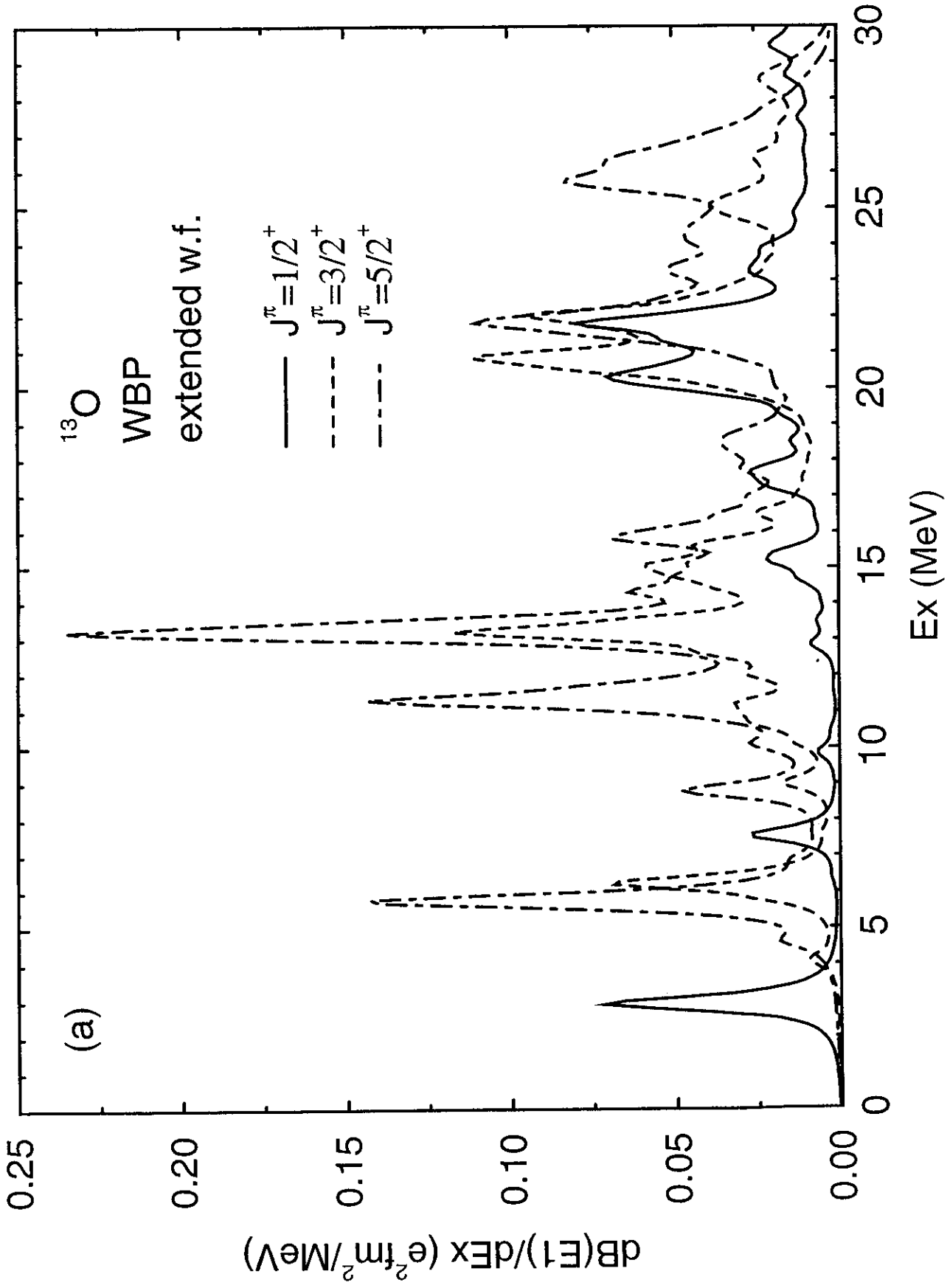
(a)
^{13}O
WBP
extended w.f.
$J^\pi=1/2^+$
$J^\pi=3/2^+$
$J^\pi=5/2^+$
dB(E1)/dEx (e^{2}fm^2/MeV)
Ex (MeV)
0.00
0.05
0.10
0.15
0.20
0.25
0
5
10
15
20
25
30

Figure 3

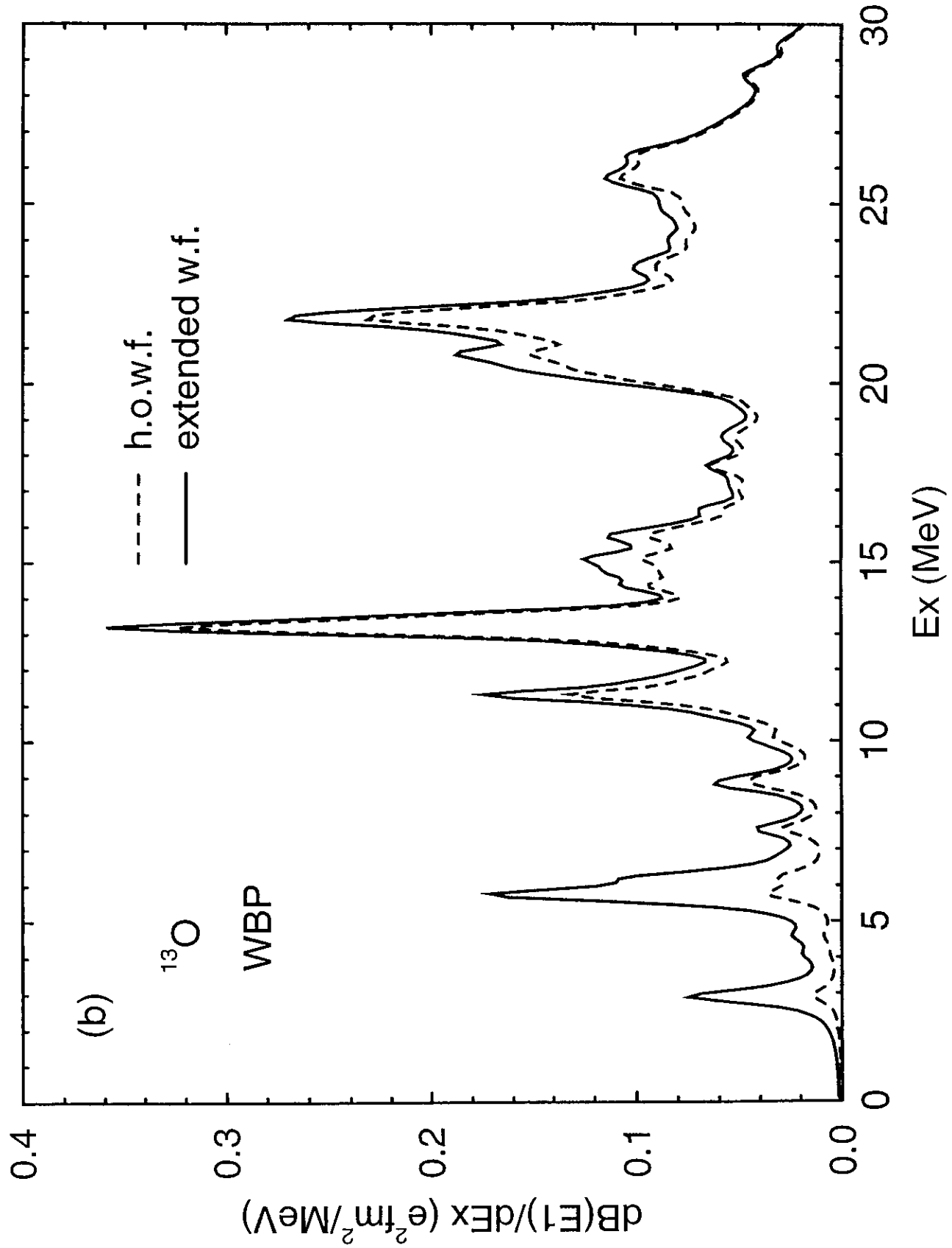
(b)
^{13}O
WBP
h.o.w.f.
extended w.f.
dB(E1)/dEx (e^{2}fm^2/MeV)
Ex (MeV)
0.0
0.1
0.2
0.3
0.4
0
5
10
15
20
25
30

Figure 4

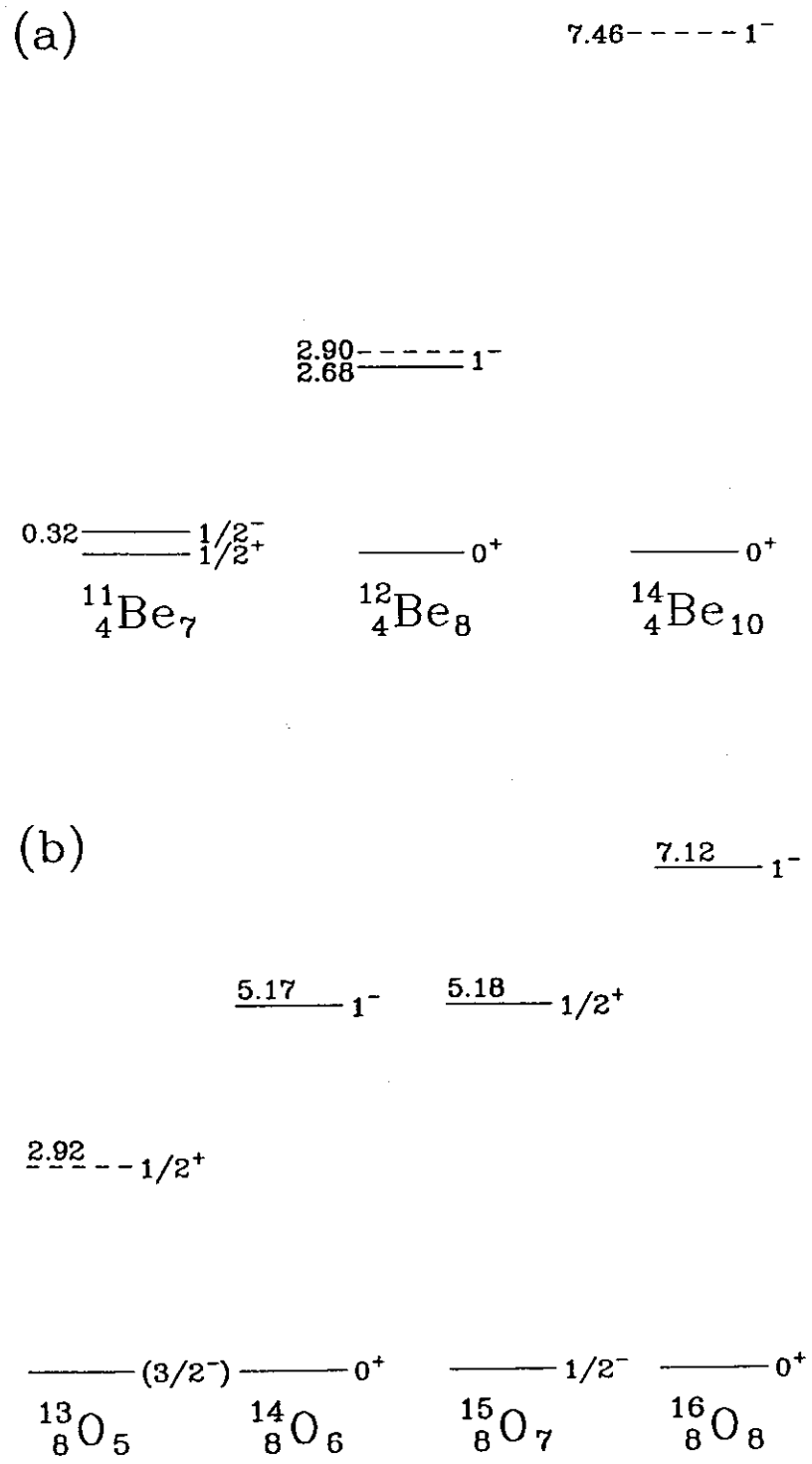
(a)
7.46 1⁻
2.90 1⁻
2.68
0.32 1/2⁻
1/2⁺
0⁺
0⁺
$^{11}_{4}Be_{7}$
$^{12}_{4}Be_{8}$
$^{14}_{4}Be_{10}$
(b)
7.12 1⁻
5.17 1⁻
5.18 1/2⁺
2.92 1/2⁺
(3/2⁻)
0⁺
1/2⁻
0⁺
$^{13}_{8}O_{5}$
$^{14}_{8}O_{6}$
$^{15}_{8}O_{7}$
$^{16}_{8}O_{8}$